Ha *et al. Applied Biological Chemistry* (2023) 66:19
https://doi.org/10.1186/s13765-023-00778-2

KSABC
The Korean Society for Applied Biological Chemistry

ARTICLE

Open Access

Antimicrobial photodynamic therapy with *Ligularia fischeri* against methicillin-resistant *Staphylococcus aureus* infection in *Caenorhabditis elegans* model

Ngoc Minh Ha[1,2†], Hoseong Hwang[1†], Seemi Tasnim Alam[1], Uyen Tran Tu Nguyen[1,2], Soon Kwang Lee[1], Jin-Soo Park[1], Jin-Chul Kim[2,3], Hak Cheol Kwon[1], Jaeyoung Kwon[1,2*] and Kyungsu Kang[1,2*]

Abstract

The high prevalence of methicillin-resistant *Staphylococcus aureus* (MRSA) infection threatens the effectiveness of current clinical settings. Antimicrobial photodynamic therapy (APDT) is a promising alternative to antibiotics for treating infections due to its low resistance. This study aimed to evaluate the antibacterial properties of APDT with *L. fischeri* extract (LFE) against MRSA and various skin and oral pathogens in vitro and its photopharmaceutical actions in *Caenorhabditis elegans*. The antimicrobial activities of APDT with LFE against pathogens were evaluated using plate counting method. The chemical profile was characterized using high-performance liquid chromatography and spectrophotometry. The growth rate assay, lifespan assay, and bacterial attachment on worms were performed to assess the therapeutics effects in *C. elegans*. The swab method was used for the detection of pathogens on the micropig skin surface. The APDT treatment with *L. fischeri* extract (LFE, 20 μg/mL) and red light (intensity of 120 W/m^2) reduced 4.3–4.9 log (colony forming unit/mL) of *Staphylococcus aureus*, MRSA, *Cutibacterium acnes*, *Streptococcus mutans*; and 2.4 log (CFU/mL) of *Candida albicans*. Chemical analysis revealed that LFE enriched three active photosensitizers. APDT reduced bacterial populations on worms, recovered growth retardation, and improved lifespan in MRSA-infected *C. elegans* without causing severe side effects. The surface eradication of MRSA after exposure to LFE with red light was demonstrated on micropig skin. These findings highlight the significance of *L. fischeri* as a natural resource for the safe phototreatment of MRSA infection in the biomedical and cosmeceutical industries.

Keywords Antimicrobial photodynamic treatment, *C. elegans*, *Ligularia fischeri*, Pheophorbide, MRSA, *Staphylococcus aureus*

† Ngoc Minh Ha and Hoseong Hwang are contributed equally to this work

*Correspondence:
Jaeyoung Kwon
kjy1207@kist.re.kr
Kyungsu Kang
kskang@kist.re.kr
[1] Natural Product Informatics Research Center, Gangneung Institute of Natural Products, Korea Institute of Science and Technology, 679 Saimdang-ro, Gangnneung, Gangwon-do 25451, Republic of Korea
[2] Division of Bio-Medical Science & Technology, KIST School, University of Science and Technology (UST), Gangneung, Gangwon-do 25451, Republic of Korea
[3] Natural Product Research Center, Gangneung Institute of Natural Products, Korea Institute of Science and Technology, Gangneung, Gangwon-do 25451, Republic of Korea

Introduction

Infectious diseases caused by methicillin-resistant *Staphylococcus aureus* (MRSA) continue to be a significant global concern. Although antibiotics are quick and effective, drug resistance in pathogenic bacteria increases the likelihood of treatment failure and economic burden [1]. Therefore, more sustainable treatment with lower resistance risk is desirable.

One of the promising options for treating microbial infection is antimicrobial photodynamic therapy (APDT). In APDT, a photoactive substance in the presence of oxygen undergoes a photochemical activation by light that absorbs and transfers energy to the oxygen molecule to generate reactive oxygen species (ROS) like singlet oxygen and superoxides. ROS has potent oxidative properties that can permanently modify cellular constituents like fatty acids, amino acids, and nucleobases that cause the elimination of harmful bacteria [2, 3]. It has several advantages, including high killing selectivity, minimal invasiveness, and a lower risk of toxicity induction in nearby host tissues due to the selective accumulation of target pathogens around the photosensitizers and the restriction of light application to a specific local area [4–6]. APDT treats infectious diseases caused by bacteria and fungi in vitro and in animal models, such as skin infections, peri-implantitis, periodontitis, and diabetic foot ulcers [4, 5, 7].

As plants are a rich source of photoactive chemicals with diverse secondary metabolite chemical groups and distinct structures that have advantages in terms of minimal side effects and economics, attempts are therefore needed for the screening of plant-derived material for APDT. *Ligularia fischeri* is a wild vegetable plant with yellow composite flowers often used in folk medicine to treat jaundice, scarlet fever, rheumatoid arthritis, and liver diseases [7]. It is known for its anti-oxidation, anti-cancer, anti-obesity, anti-hepatotoxic, and anti-inflammation properties [8]. However, no study has used this plant as a photodynamic antimicrobial material and evaluated its therapeutic impact on *C. elegans*.

In this study, *Caenorhabditis elegans* was used as a model to evaluate the impact of ADPT with LFE. Thanks to the short lifespan and high percentage of genes that are homologous to human genes; this invertebrate nematode has proven to be a useful model for the screening of bioactive compounds in therapeutic fields involving antiaging, antineurodegeneration, gut health improvement, and metabolic disorders [9–18]. Regarding pathogen infections, live-*C. elegans* infection model was established to evaluate the in vivo efficacy against bacteria *Enterococcus faecalis*, *Streptococcus pyogenes*, *Staphylococcus aureus*, and fungi *Candida albicans* [19–23]. Here, it is the first time APDT with LFE was evaluated and its therapeutic impacts was illustrated on *C. elegans*.

The present investigation aimed to evaluate the anti-infective effects of LFE in combination with red light against different pathogenic microorganisms, particularly MRSA in vitro. The therapeutic effects of APDT treatment against MRSA infection were further assessed in *C. elegans* model. Figure 1 illustrates the experimental scheme of the study.

Methods

Sample collection

The LFE for rapid screening was provided from the natural product library, Korea Institute of Science and Technology, Gangneung Institute of Natural Products (Accession number KHG2016-01-0007; Gangwon-do, South Korea). Dried *L. fischeri* was purchased from the herbal market in Jeongseon (Gangwon-do, South Korea).

Extraction and compound isolation

The *L. fischeri* samples were dried (900 g) and ground, and 101.1 g of dark green extract was collected under 2-hour-reflux with ethanol (9 × 2 L), followed by filtration and evaporation at low pressure. Bioassay-guided fractionation scheme was applied for the isolation of

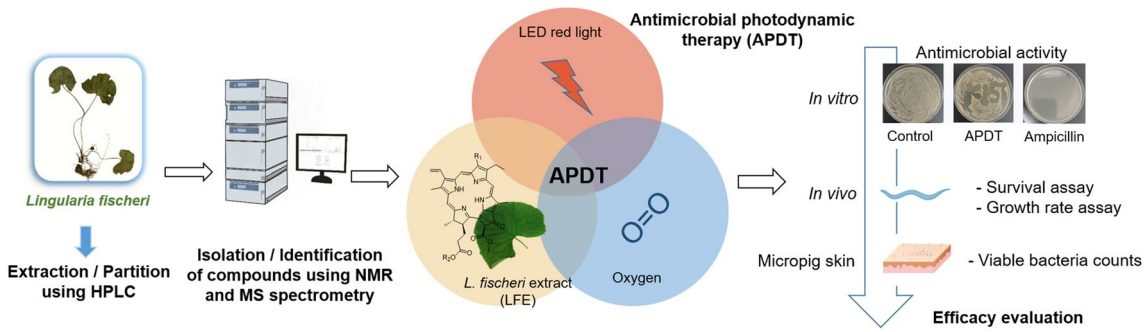

Fig. 1 Experimental scheme of the present study, antimicrobial photodynamic therapy (APDT) with *Ligularia fischeri* extract (LFE)

bioactive substances. The screening method was used to detect the singlet oxygen generation ($^1O_2$). LFE (14.5 g) was adsorbed on Celite, separated by a column filled with Diaion HP-20 resin (130 g, 2.5 × 18 cm) and eluted with ethanol/water/acetone (3:2:0, 4:1:0, 1:0:0, and 0:1:1). The four fractions ranged from F1 to F4. F4 (215.1 mg) were separated by a Gilson semipreparative high-pressure liquid chromatography (HPLC, Phenomenex Luna 10 µm C_{18} (2) column [10 µm, 250 × 21.2 mm]) and eluted using gradient conditions (acetonitrile/water, 77:23 to 3:97 in 120 min, flow rate 8 mL/min, 420 nm) to collect compounds **1** (1.6 mg, t_R = 36.1 min), **2** (2.7 mg, t_R = 57.8 min), and **3** (1.6 mg, t_R = 65.4 min).

Structural identification of active compounds

The chemical structures of compounds **1**–**3** were identified using a combination of spectroscopy and spectrometry analysis (Nuclear magnetic resonance [NMR]: Varian 500 MHz NMR spectrometer; HPLC-MS: Agilent 1200 HPLC and a 6120 quadrupole mass spectrometry [MS] with a Phenomenex Luna C_{18} (2) column [5 µm, 250 mm × 10 mm]). The NMR and MS data of compounds **1**–**3** are appended in the Supplementary material.

Ultra-performance liquid chromatography (UPLC) analysis

Waters Acquity H-Class system (Waters, Milford, MA, USA) was used to analyze the sample. Column separation (Phenomenex Kinetex XB-C18 column, 2.6 µm, 100 mm × 2.1 mm) was conducted at a detection wavelength of 420 nm. Two µL of sample was injected and the column temperature was remained stable at 30 °C. After elution from the column, the extract and the isolated compounds were dissolved in 1 mL of internal standard 10 µg/mL. The calibration curves were made from at least five different concentrations of the compounds. The intra- and inter-day precision and accuracy were estimated by analyzing at least three replicates within a single day and on five subsequent days, respectively. Quantification and validation experiments of compounds **2** and **3** were performed using only compound **2** because both compounds are stereoisomers.

Singlet oxygen generation assay

The singlet oxygen ($^1O_2$) generation was measured through the imidazole-RNO (*N*,*N*-dimethyl-4-nitrosoaniline) method [19]. In brief, mixtures of RNO 0.25×10^{-4} M and l-histidine 0.125×10^{-1} M was prepared in sodium phosphate buffer 0.25×10^{-1} M (pH 7.0) and then aliquoted into a 96-well plate. Plates were prepared by dissolving samples in water–dimethyl sulfoxide (DMSO) mixtures (1:1) and then subjected to red light (655 nm wavelength, S-Tech light emitting diode (LED)) at the intensity of 200 W/m^2 for 30 min. The $^1O_2$ production was recorded at 440 nm. A DMSO-water mixture was served as a negative control.

Bacterial strains and bacterial suspension preparations

Cutibacterium acnes KCTC3314, *Staphylococcus aureus* KCTC3881, *Candida albicans* KCTC7965, and *Streptococcus mutans* KCTC3065 strains were purchased from the Korean Collections for Type Cultures (Jeongeup, Korea). *Pseudomonas aeruginosa* PAO1 was purchased from American Type Culture Collection, and MRSA 2659 was acquired as described previously [20]. Luria-Bertani (LB) broth was used to culture MRSA, *S. aureus*, *S. mutans*, *P. aeruginosa*, and Sabouraud broth was used to culture *C. albicans*. *C. acnes* was grown in brain heart infusion (BHI) broth. The bacterial suspensions were prepared by diluting fresh cultures with the corresponding liquid broth and incubating at 37 °C overnight. Bacterial suspensions were adjusted to an optical density of 0.01 at 600 nm for APDT treatments. The initial bacterial cell numbers were determined as described earlier [19].

APDT against various pathogenic microorgansims in vitro

In vitro APDT assays were conducted with LED red light (660 nm wavelength). The light intensity was determined by a radiometer (LI-250 A LICOR, Bioscience). Extract (20 µg/mL or 50 µg/mL) or fractions (20 µg/mL) or isolated compounds (10 µg/mL) were added to bacterial suspensions and incubated at 25 °C for 30 min (*S. aureus*, MRSA, *S. mutans*, and *C. acnes*) or 1 h (*P. aeruginosa* and *C. albicans*). After incubation, 100 µL bacterial suspension was aliquoted in a transparent 96-well plate (SPL Life Science, Pocheon, Korea) and subjected to LED red light at 120 W/m^2 from the top for 15 min. APDT against *P. aeruginosa* and *C. albicans* was performed at 600 W/m^2. After 24-48 h incubation, CFU was determined and expressed in log (CFU/mL). Ampicillin, vancomycin, or gentamycin (100 µg/mL) was used as a positive control for bacteria, and nystatin (20 µg/mL) was used as the anti-fungal positive control. At least three independences were performed in all experiments.

C. elegans maintenance

Wild-type *C. elegans* N_2 were purchased from the Caenorhabditis Genetics Center (Minneapolis, MN, USA). *C. elegans* was maintained on a nematode growth medium (NGM) agar plate at 20 °C supplied with *E. coli* OP50. Egg synchronization was prepared as described previously [18].

Growth rate assay in *C. elegans* after APDT

The pathogen preparation and toxicity test under two conditions (pathogen-prefed and infected *C. elegans*) were conducted as described previously [19]. Briefly, in

the prefeeding model, MRSA or *S. aureus* KCTC3881 suspension was treated with LFE-APDT under red light (120 W/m^2, 15 min) and then was coated on an NGM plate and fed to *C. elegans* eggs. The body length was measured after 96 h using a stereoscopic microscope. In the infection condition, the eggs were fed MRSA or *S. aureus* and LFE until reaching the L1 stage. Infected worms were subjected to red light (600 W/m^2, 10 min) and recorded the body length on the fourth day from the egg stage.

In vivo APDT efficacy test in the MRSA-infected *C. elegans* model

Adult worms were incubated in MRSA suspension (400 µL, OD = 0.1) for 24 h at 20 °C in a 24-well plate. After the infection, the wells were incubated with LFE (20 µg/mL, 30 min) in a shaker. Control was incubated with DMSO. Then, 50 worms were allowed to crawl in blank plates twice to remove the excess MRSA in the platinum wire. The final NGM plate was irradiated at 600 W/m^2 for 5 min. Five worms from each treatment plate were moved to 0.5 mL LB broth and samples were spread on LB agar plates. The reliability of this assay was tested as described previously. It was illustrated that the number of bacteria on the platinum wire or NGM plate were insignificant compared to that on the *C. elegans* body [19]. Survivability was also evaluated after APDT treatment by transferring to blank NGM plates and monitoring the number of living, dead, and censored worms every day [14].

Removal of the MRSA from the micropig skin surface

Micropig skin was purchased from APURES Co., Ltd. (Gyeonggi-do, South Korea). Prior to the experiment, the skin was sterilized with 70% ethanol, followed by UVA exposure for 15 min. Fresh MRSA or *C. acnes* suspension (OD 0.01) mixed with or without LFE (20 µg/mL) was spread on the micropig skin at 5 µL/cm^2. Ampicillin (100 µg/mL) was served as a positive control. The coated skin was irradiated under red light (20 W/m^2, 30 min). The skin in each treatment group was stamped on LB or BHI agar and incubated for 48 h. After treatment, the bacterial load on the skin was determined using the swabbing method as described previously [18].

Statistical analysis

Data were analyzed using GraphPad Prism 7.0 (La Jolla, CA, USA). Statistical analysis of lifespan assay was conducted with JMP software (version 10, SAS Institute, Cary, NC, USA) using the log-rank test. A value of $p < 0.05$ was considered statistically significant. The data are presented as the means ± SD, and experiments were performed in duplicates or triplicates with at least three independences.

Results

LFE as a novel active photosensitizer based on the singlet oxygen generation assay

Fifty different ethanol extracts of plants (Natural product library, KIST) were rapidly screened for their ability to generate $^1O_2$ (red light was used since long-wavelength is sufficient for penetration and safety of APDT [19, 24, 25]), among which LFE showed the best activity (Additional file 1: Figure S1), and then the fractionation (F1–F4) from LFE was performed for further identification of the photoactive compounds.

In vitro APDT effect with LFE

APDT with LFE inhibited the growth of various pathogens in vitro

LFE or red light alone did not suppress bacterial growth, showing that the current light dose or LFE was not hazardous to bacterial cells (Fig. 2). APDT treatment, on the other hand, considerably reduced the growth of all gram-positive bacteria tested, with log reductions of 4.5, 4.7, 4.9, and 4.3 of viable cells of *S. aureus*, MRSA, *S. mutans*, and *C. acnes*, respectively. The log decrease achieved by the APDT with LFE against *S. aureus*, MRSA, and *S. mutans* was 2.2-, 2.3-, and 7.0-fold greater than the antibiotic therapy. Pathogenic fungi *C. albicans* reduced viable cells by 2.4 log (CFU/mL), which was 0.5 log lower than the nystatin therapy. With a 0.8 log decrease, APDT had a weak effect against gram-negative *P. aeruginosa*.

APDT with LFE under different light conditions in vitro

The APDT effect with LFE against MRSA was investigated to validate the applicable range of APDT conditions with different doses of red light. At the milder light intensity 20 W/m^2, APDT LFE showed sufficient antimicrobial activities (Fig. 3). Light exposure of photo materials for 30 min reduced 3.7 log (CFU/mL). LFE was effective after 10 min of exposure, inhibiting cell growth by 3.0 log (CFU/mL) reduction. APDT with 1 W/m^2 red light for 10 min had a weak antibacterial action against MRSA, with the log decrease of 0.3 (data not shown).

Identification of photoactive compounds for the standardization of LFE

Compound identification of LFE

Although F3 fraction generated slightly higher singlet oxygen than those by LFE or other fractions (Additional file 1: Figure S2), only LFE and F4 were analyzed using UPLC–PDA to identify photoactive compounds after carefully considering the yield and activity of LFE and

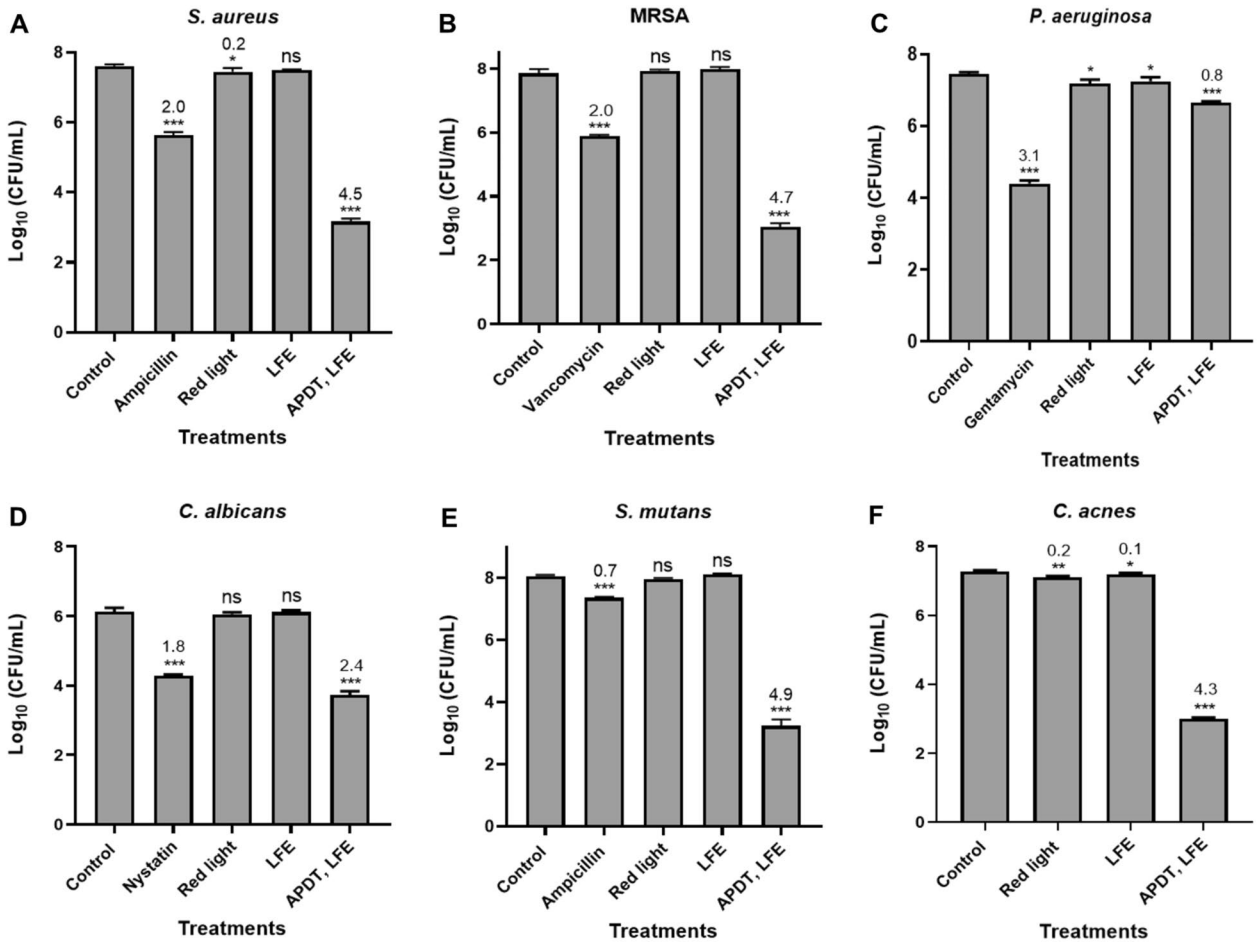

Fig. 2 In vitro antimicrobial activities of APDT with LFE against various pathogens. **A** APDT against *S. aureus* KCTC3881 (30 min incubation; red light intensity at 120 W/m^2 for 15 min), **B** APDT against MRSA (30 min incubation; red light intensity at 120 W/m^2 for 15 min). **C** APDT against *P. aeruginosa* (60 min incubation; red light intensity at 600 W/m^2 for 1 h). **D** APDT against *C. albicans* (60 min incubation; red light intensity at 600 W/m^2 for 15 min). **E** APDT against *S. mutans* (30 min incubation; red light intensity at 120 W/m^2 for 15 min). **F** APDT against *C. acnes* (30 min incubation; red light intensity at 120 W/m^2 for 15 min). Suspensions of *S. mutans*, MRSA, *S. aureus*, and *C. acnes* were treated with LFE (20 μg/mL); *P. aeruginosa* and *C. albicans* were treated with LFE (50 μg/mL). Nystatin (20 μg/mL) and vancomycin or ampicillin (100 μg/mL) were used as positive controls. The data are expressed as mean ± standard error (n = 2), and representative of at least two independences. ns indicates no statistical significance relative to the control group. Significant differences are expressed with * for $p < 0.05$, ** for $p < 0.01$, and *** for $p < 0.001$ relative to the vehicle control. The log reductions compared with vehicle control are presented in each column

fractions in vitro (Additional file 1: Figure S3). Three main peaks were detected in the chromatogram at 420 nm (Fig. 4A), showing characteristic UV absorption around 420 and 660 nm due to highly conjugated π-electron systems. The chemical database metabolite annotation using *m/z* values showed that these compounds might contain a porphyrin skeleton.

Three compounds (**1** − **3**) were isolated using various chromatographic techniques (Fig. 4B). Among them, compound **2**, which had the molecular formula of $C_{35}H_{36}N_4O_5$ according to mass spectrum, was the most abundant. The ^{1} H NMR data of compound **2** showed a characteristic signal pattern of the cyclic tetrapyrrole core structure (δ_H 9.52, 9.40, and 8.56) with additional olefinic proton signals (δ_H 7.99, 6.29, and 6.18). Furthermore, it had five different methyl signals (δ_H 3.68, 3.40, 3.24, 1.81, and 1.69). This data was similar to that of pheophorbide a. The ^{1} H NMR data and the *m*/*z* value of compound **3** were superimposable to that of compound **2**. Previous literature have shown that compound **3** was considered 21-*epi*-pheophorbide a [19]. According to mass data, the molecular formula of compound **1** was $C_{35}H_{34}N_4O_6$. Data also showed a characteristic signal pattern of the cyclic tetrapyrrole core structure (δ_H 10.44, 9.72, and 8.55).

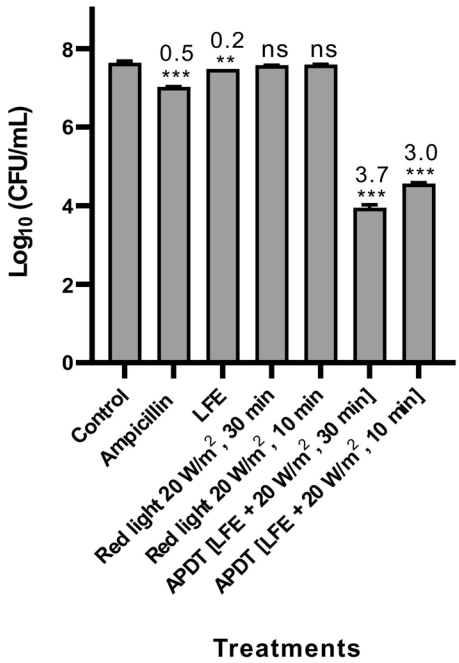

Fig. 3 In vitro antimicrobial activities of LFE under different light conditions. APDT with LFE (20 μg/mL; incubation time, 30 min) against MRSA under a red light intensity of 20 W/m^2 for 10 or 30 min. Ampicillin (100 μg/mL) was used as the positive control. The data are expressed as mean ± standard error (n = 2) and representative of three independences. ns indicates no statistical significance relative to the control group. Significant differences are expressed with ** for $p < 0.01$ and *** for $p < 0.001$ relative to the vehicle control. The log reductions compared with vehicle control are presented in each column

However, an aldehyde proton signal (δ_H 11.20) and four methyl signals were only displayed. Therefore, compound **1** was deduced as pheophorbide b [19].

Pheophorbides as active compounds for the APDT effects

All three pheophorbide-related compounds isolated from LFE significantly suppressed the growth of *S. aureus*, with the log reduction of 3.9, 3.8, and 3.6 for compounds C1-C3, respectively (Fig. 4C).

Quantitative analysis of LFE

The bioactivity analysis of LFE showed that the three active compounds potentially contribute to its APDT activity. Next, we performed quantitative chemical analysis for the standardization of LFE and its APDT quality control. For the chemical analysis of LFE, the UPLC–PDA method was developed, where dimethyl curcumin was used as the internal standard. The established method was then validated to check the specificity, linearity, accuracy, and precision, suggesting this method is reliable (Table 1). The quantitative analysis (w/w) suggested the amounts of compounds **1**−**3** as 0.22% ± 0.01% (**1**), 0.47% ± 0.01% (**2**), and 0.07% ± 0.01% (**3**), respectively. The experiments were carried out in triplicates. From these results, we concluded that LFE could be a valuable photosensitizer candidate due to the abundance of photoactive compounds, potentially leading to effective APDT.

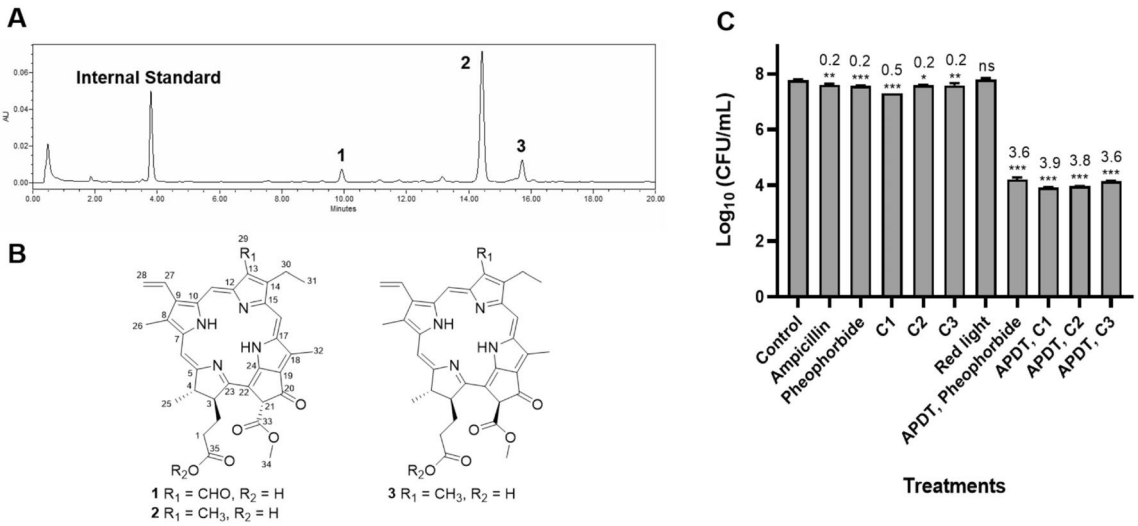

Fig. 4 Chemical profiling of LFE. **A** UPLC–PDA chromatogram of LFE. **B** The chemical structures of isolated compounds **1**−**3**. **C** Antimicrobial activities against *S. aureus* KCTC3881 of isolated compounds C1–C3. APDT with isolated compounds (10 μg/mL; incubation time, 30 min) against *S. aureus* under red light (20 W/m^2; 30 min). Ampicillin (100 μg/mL) and APDT with pheophorbide were used as positive controls. The data are expressed as mean ± standard error (n = 2) and representative of three independences. ns indicates no statistical significance relative to the control group. Significant differences are expressed with * for $p < 0.05$, ** for $p < 0.01$, and *** for $p < 0.001$ relative to the vehicle control. The log reductions compared with vehicle control are presented in each column

Table 1 Linearity, accuracy, and precision of results (n = 3)

No	Linear range	Regression equation	r^2	Precision (%RSD)		Accuracy	
	(μg/mL)			Intra-day	Inter-day	Intra-day	Inter-day
1	6.3–100.0	y = 0.0023x–0.0036	0.999	1.1 ± 1.0	1.2 ± 1.0	101.0 ± 3.2	100.9 ± 3.3
2	6.3–100.0	y = 0.0152x–0.0148	0.999	0.8 ± 0.3	0.6 ± 0.3	97.5 ± 0.8	96.5 ± 0.4

APDT with LFE in the *C. elegans* model

Effects of APDT on the growth rate of the S. aureus and MRSA-infected C. elegans

Based on the in vitro results, the therapeutic effects of considerable pathogen eradication were examined using key physiological parameters in the *C. elegans*. The efficacy and side effects of APDT were first evaluated in vivo using the standardized LFE in two different pathogen-infected *C. elegans* models.

In the prefeeding model, worms were supplied with APDT or ampicillin-treated pathogens in NGM plate. During *S. aureus* infection, worms treated with APDT with LFE could decrease growth retardation effects, with the body length of 1,057 mm, which was similar to the vehicle control and ampicillin treatment (1,083 mm and 1,121 mm, respectively) (Fig. 5A, B). After 4 days, the body length of worms fed with untreated MRSA decreased significantly (0.53-fold of the vehicle control, $p < 0.001$). The MRSA-induced decrease in the worm size was recovered using ampicillin by only 13.11%, whereas APDT treatment using LFE could significantly increase the growth by 71.98% compared with the MRSA-infected worms (Fig. 5C, D).

In addition, we determined the APDT efficacy in the infection model, which is a more reliable experimental model [19]. APDT treatment at the L1 stage in the infection model with MRSA or *S. aureus* showed a detrimental effect on the growth rate of worms. Worm treated with APDT using LFE against *S. aureus* recovered to 1,027 mm of body length, which is similar to that of control healthy worms (1,074 mm) (Fig. 6A , B). Regarding MRSA, the infection caused considerable decrease in the body length of infected worms compared with that of healthy worms in the vehicle control (693 mm and 1,019 mm, respectively). Notably, ampicillin treatment could not rescue the growth retardation caused by MRSA at all, whereas APDT treatment significantly increased the growth, with the mean worm length of 930 mm, which was 237 mm longer than that of the MRSA-infected worms (Fig. 6C, D).

In the prefeeding and infection *C. elegans* models, ampicillin treatment was only effective against *S. aureus*, whereas APDT with LFE could alleviate the toxic effects on body length caused by *S. aureus* and MRSA, indicating its promising therapeutic effects in antibiotic-resistant bacterial infection.

Effects of APDT on survivability of C. elegans under MRSA infection

Next, we evaluated the effects of APDT on the survivability of the MRSA-infected worms, because survivability is the most reliable indicator of the therapeutic effect and side effects of the antimicrobial treatment [19]. MRSA killed worms (n = 25) within 8 days (Fig. 7A), and the single treatment of red light or LFE did not affect the lifespan of the MRSA-infected worms. However, after the APDT treatment of LFE and red light, the survival rate of worms was extended, with a mean lifespan of 4.72 ± 0.25 days, significantly different from the MRSA-infected worms (3.88 ± 0.20 days, $p = 0.0078$). The number of worms-associated pathogenic bacteria was also assessed (Fig. 7B). During the infection, number of MRSA associated with worm was 9700 ± 300 (CFU/worm); in contrast, after APDT treatment, the number of pathogen on worms reduced remarkably to 10 ± 2 (CFU/worm). Similar significant antimicrobial effects were also observed in *C. elegans* infected with normal *S. aureus* KCTC3881 following APDT treatment (Additional file 1: Figure S4). These results indicate that the killing of MRSA by APDT helped to cure *C. elegans* against infection.

Eradication of MRSA and *C. acnes* load on micropig skin by LFE-APDT

APDT efficacy was tested to eradicate MRSA or *C. acnes* from micropig skin and to evaluate its biomedical potential for infective skin diseases. The inoculation of MRSA on micropig kin was about 5.8 log (CFU/cm^2) (Fig. 8A, B). This bacterial load slightly reduced under the sole treatment of ampicillin or LFE, with the log reduction of 0.5 and 0.1 respectively. When a combination of red light and LFE was used, the MRSA concentration on the skin was significantly reduced by 3.4 log (CFU/cm^2) compared to the control. Similarly, the APDT LFE inhibited the *C. acnes* growth on skin, with the log reduction of 2.5, which was 2.1 log lower than the ampicillin treatment (Fig. 8C, D).

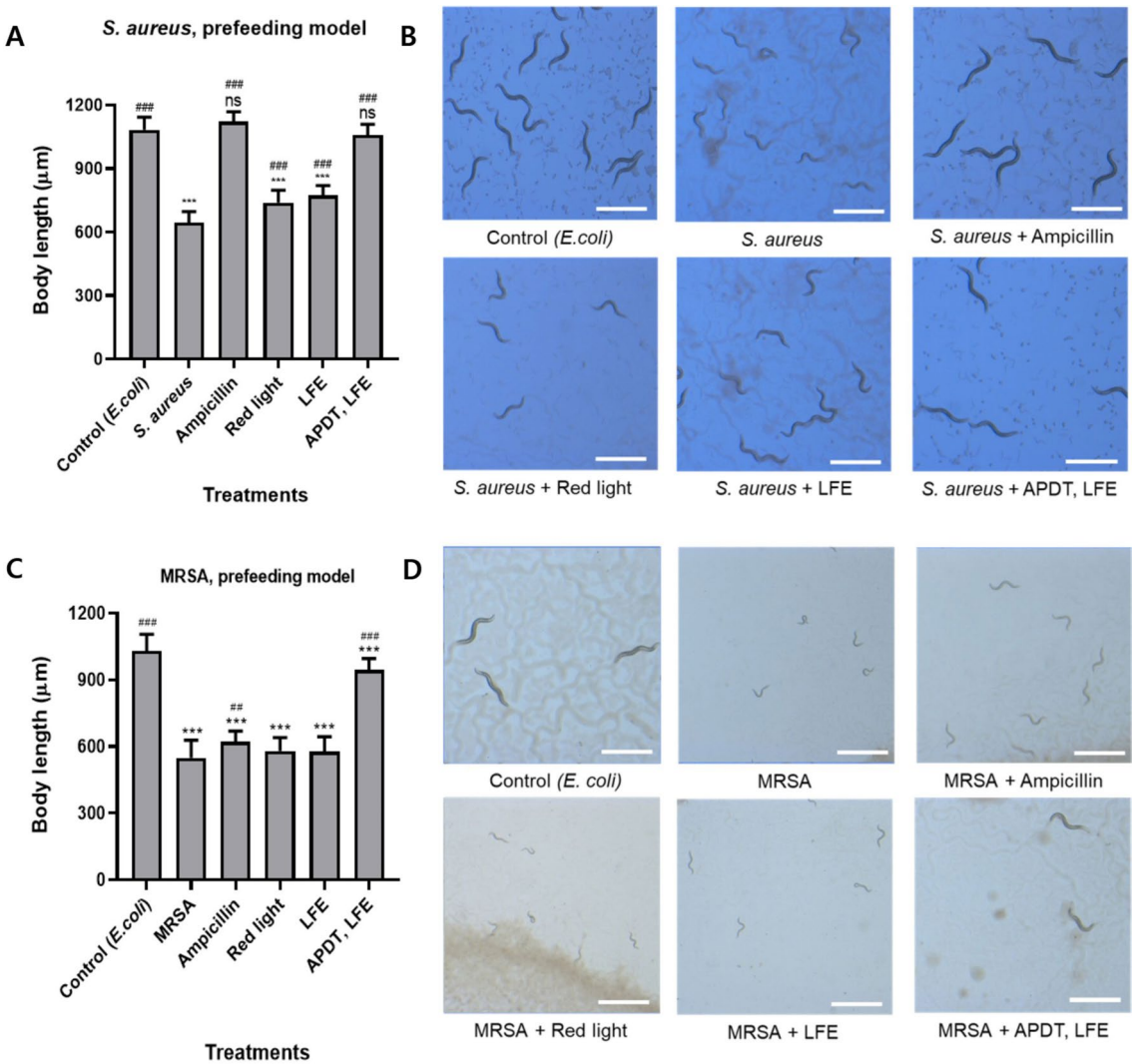

Fig. 5 Effect of APDT-LFE on the growth of *C. elegans* in the prefeeding model. *S. aureus* KCTC3881 or MRSA was pretreated with APDT using LFE (20 µg/mL; 30 min incubation) and red light 120 W/m^2 for 15 min. The treatment with ampicillin (100 µg/mL) served as the positive control. Synchronized eggs were fed with *E. coli* OP50 as vehicle control, or treated MRSA or *S. aureus* with APDT or ampicillin. The body length **A**, **C** and the microscopic images of the worms **B**, **D** were evaluated four days after the egg state. White scale bar = 1 mm. The data are representative of three independent experiments. Analysis of variance test (n = 20). ns indicates no statistical significance relative to the control group; significant differences are expressed with *** for $p < 0.001$ relative to the vehicle control group; ## for $p < 0.01$, ### for $p < 0.001$ relative to the pathogen single treatment group

Discussion

Human infectious disorders are strongly linked to temporal dysbiosis caused by specific pathogenic bacteria. The bacteria tested in this study have been reported to be opportunistic pathogens of humans and the primary drivers of skin and dental diseases [26, 27]. Among them, MRSA is one of the most common antibiotic-resistant bacterial strains, posing threat in the treatment of soft tissue and skin infections in systemic diseases, including toxic shock syndrome in the community and healthcare settings [28]. The in vitro results demonstrated that the combination of LFE and red light with a wide range of intensity exhibited strong anti-infective effects due to the strong ROS production, causing the reduction of bacterial load higher than 3 log (CFU/mL), which is more effective than antibiotics treatments.

Our chemical study confirmed the high amount of photosensitizers, which aided in chemical profiling and standardization for future clinical approval. The photoactive ingredient in LFE was discovered to be pheophorbide, a metabolic breakdown product of chlorophyll. This is a promising photosensitizer with gold standard

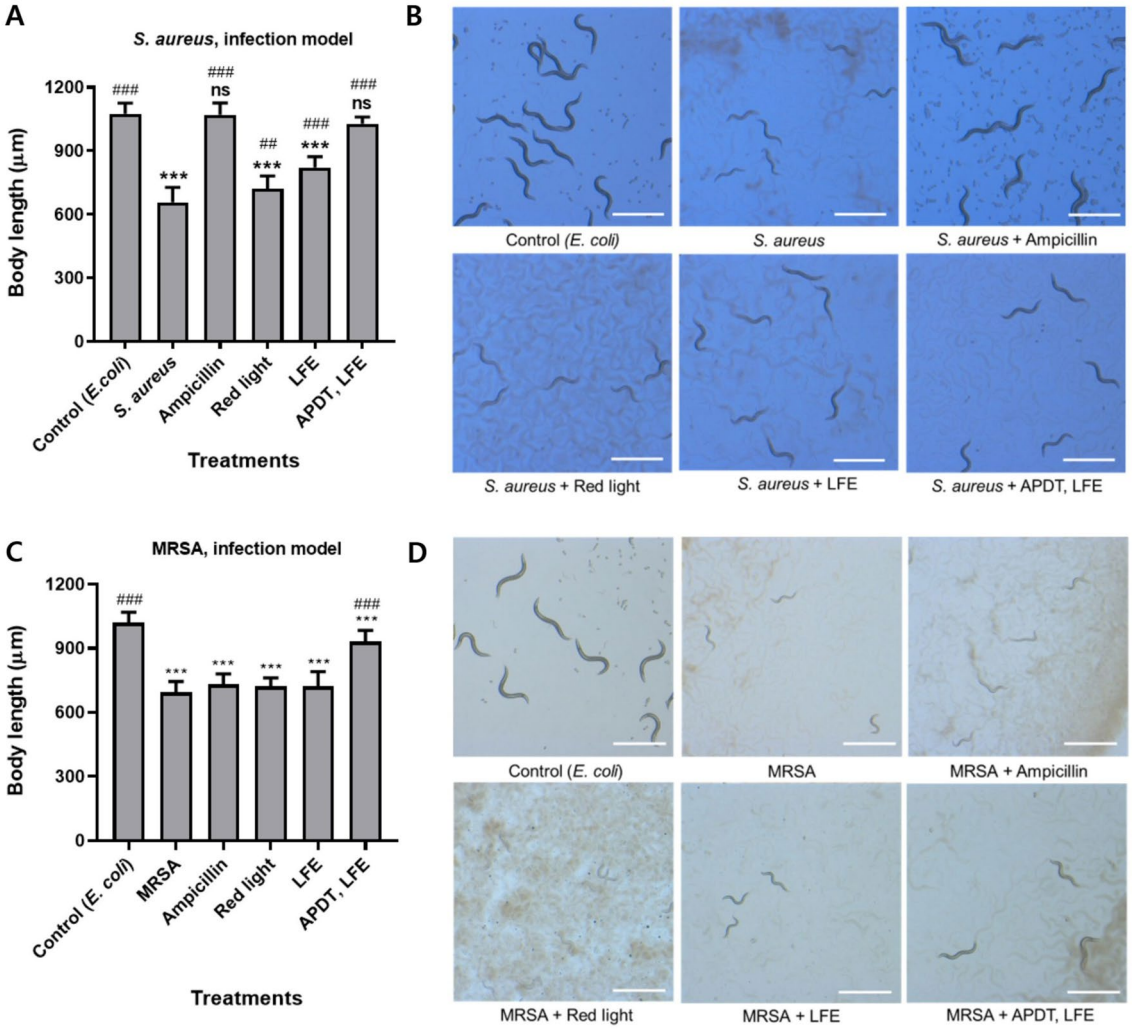

Fig. 6 Effect of APDT-LFE on the growth rate of *C. elegans* in MRSA and *S. aureus* infection model. Eggs were fed with LFE-incubated MRSA or *S. aureus* (LFE concentration:20 µg/mL; incubation time: 30 min) or ampicillin as the positive control. NGM plate coated with *E. coli* was used as vehicle control. After reaching the L1 stage, the plates were irradiated with a red light at 600 W/m^2 for 10 min. The body length **A**, **C** and the microscopic images of the worms **B**, **D** were evaluated on the fourth day after the egg state. The results are representative of three independent experiments. White scale bar = 1 mm. Analysis of variance test (n = 10). ns indicates no statistical significance relative to the control group; significant differences are expressed with *** for $p < 0.001$ relative to the vehicle control group; ## for $p < 0.01$, ### for $p < 0.001$ relative to the pathogen single treatment group

photophysical and photobiological properties such as near infrared light absorption, high singlet oxygen yield (through both the type I and type II photoprocesses with the extended π-π conjugated system), better selectivity (in microorganism cells compared to mammalian cells), and photostability, which maintains a long life at excited state during irradiation [29–32]. Furthermore, owing to the biosynthetic relation to the protoporphyrin IX present in higher organisms, biocompatibility such as pharmacokinetic clearance is anticipated [32]. Many pieces of research have shown that APDT of tetrapyrrole-based chemicals, such as porphyrins, chlorins, and their derivatives, can be used to treat skin, oral, and surface disinfection. *S. aureus, C. albicans*, and *Artemia salina* were killed by pheophorbide concentrations ranging from 20 to 100 µg/mL combined with 6 J/cm^2 of light [32]. The viable cells of *C. albicans* were deemed 3.67 ± 0.18 log(CFU/mL) under the APDT treatment of porphyrin derivatives and LED at 440–460 nm [33]. A clinical investigation conducted by Song and colleagues showed that the phototherapy of chlorophyll-a with blue light (λmax = 430 nm) and red light (λmax = 660 nm) under radiance influence of 1800 and 1170 J/cm^2 improved the inflammatory states in *Acnes vulgaris* [34]. Unlike prior

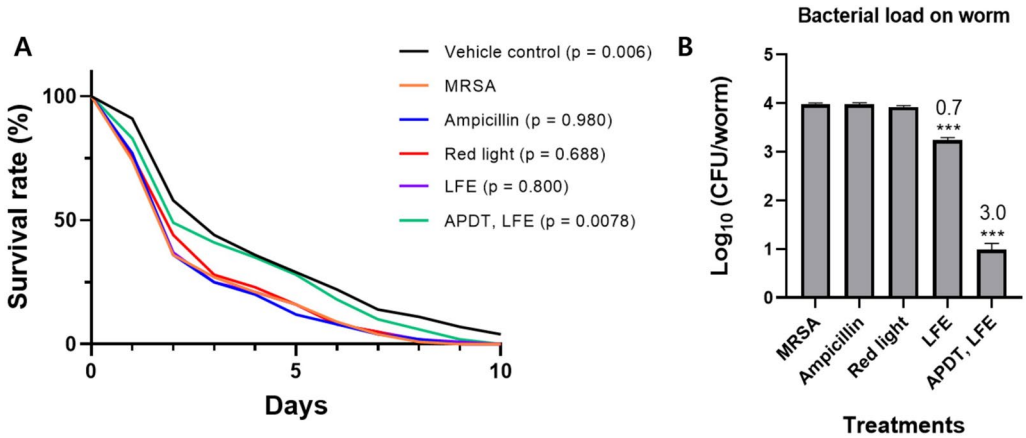

Fig. 7 Effects of APDT efficacy on lifespan **A** and bacterial attachment **B** in MRSA-infected *C. elegans*. Adult worms were incubated with fresh MRSA suspension for 24 h. Then, LFE (20 µg/mL) was treated for 30 min. DMSO was used as the control group. Next, the worms were allowed to crawl to blank NGM agar twice before the irradiation to red light at 600 W/m^2 for 5 min. The worms were then assessed for survival rate every day (**A**). The p-value according to the MRSA single treatment is presented. The data are representative of three independent experiments. Five worms from each treatment plate were also moved to fresh LB broth and spread onto LB agar for CFU determination of viable bacteria associated with *C. elegans* (**B**). The data are reported as mean ± standard error of duplicates and representative of three independent experiments. ns indicates no statistical significance relative to MRSA; significant differences are expressed with *** for $p < 0.001$ relative to MRSA. The log reductions compared with MRSA are presented in each column

studies, we used the plant *L. fischeri* as a new photosensitizer source instead of single compounds as photosensitizers. Our study first demonstrated the APDT efficacy of this food plant, especially against life-threatening MRSA. The synthesis of high-purity compounds is usually laborious and more expensive, while the usage of natural plant extract is simple, ecofriendly, and cost effective [35, 36]. The bioactive constituents in extracts may contribute to the synergistic therapeutic effects [20]. Phytochemical investigation of this plant revealed that some constituents like caffeoylquinic acids and quercetin derivatives exerted the antioxidant, anti-inflammatory activities and inhibited elastase, tyrosinase, which offered the anti-wrinkle effects [8, 37].

In our in vitro investigation, we discovered that APDT therapy for effectively controlling fungi *C. albicans* required a longer incubation time and a higher light intensity than gram-positive bacteria. Glycoproteins, soluble and insoluble polymers embedded in the membrane, large cell size, and the presence of the nuclear membrane are some factors that cause photosensitizers to take longer pre-irradiation time to penetrate the cells [38]. Previous investigations have shown that higher light energy and photosensitizer doses of methylene blue, rose bengal, and a chlorin(e6) conjugate are required to kill *C. albicans* more effectively than bacteria [38, 39]. However, LFE showed weak effectiveness in the inactivation of gram-negative *P. aeruginosa*. The hydrophobicity of the pheophorbides, the repulsion between the carboxylate group, and the additional negative charge on gram-negative membranes contribute to this limitation [31, 32]. The unfavorable result has been observed in previous studies, which encourages the development of new strategies to improve efficacy against gram-negative bacteria, such as combining different photosensitizers, conjugating inorganic salts and antibiotics, or the development of nanodelivery systems [20, 40].

As light dosimetry is a critical aspect of the success of APDT, our study emphasizes the range of photodynamic conditions for sustained light-inactivation effect from high to mild red light intensity. Our research demonstrated that the initial light energy of 120 W/m^2 against bacteria and 600 W/m^2 against fungi is the safe dose in vivo testing without harming the growth rate and reproduction of *C. elegans* [19]. APDT with light intensity of 120 and 20 W/m^2 showed antimicrobial activities against MRSA. Milder intensity 20 W/m^2 may be more suitable for commercial use, particularly in cosmeceutical therapy such as LED masks. It is worth noting that the LED red light utilized as the source for photodynamic action is not only coherent with maximum light absorption at 660 nm [41] but also minimizes the toxicity of light to local tissue and penetrating deeply into tissues [24, 25]. While blue light only reaches the stratum corneum, the red light can penetrate the stratum corneum and hair follicles, enabling the killing effects on the external surface and inactivating the virulent factors such as extracellular enzymes by dermatophytes [42].

In *C. elegans*, APDT treatment improved illness conditions by reducing the number of bacteria adhered to

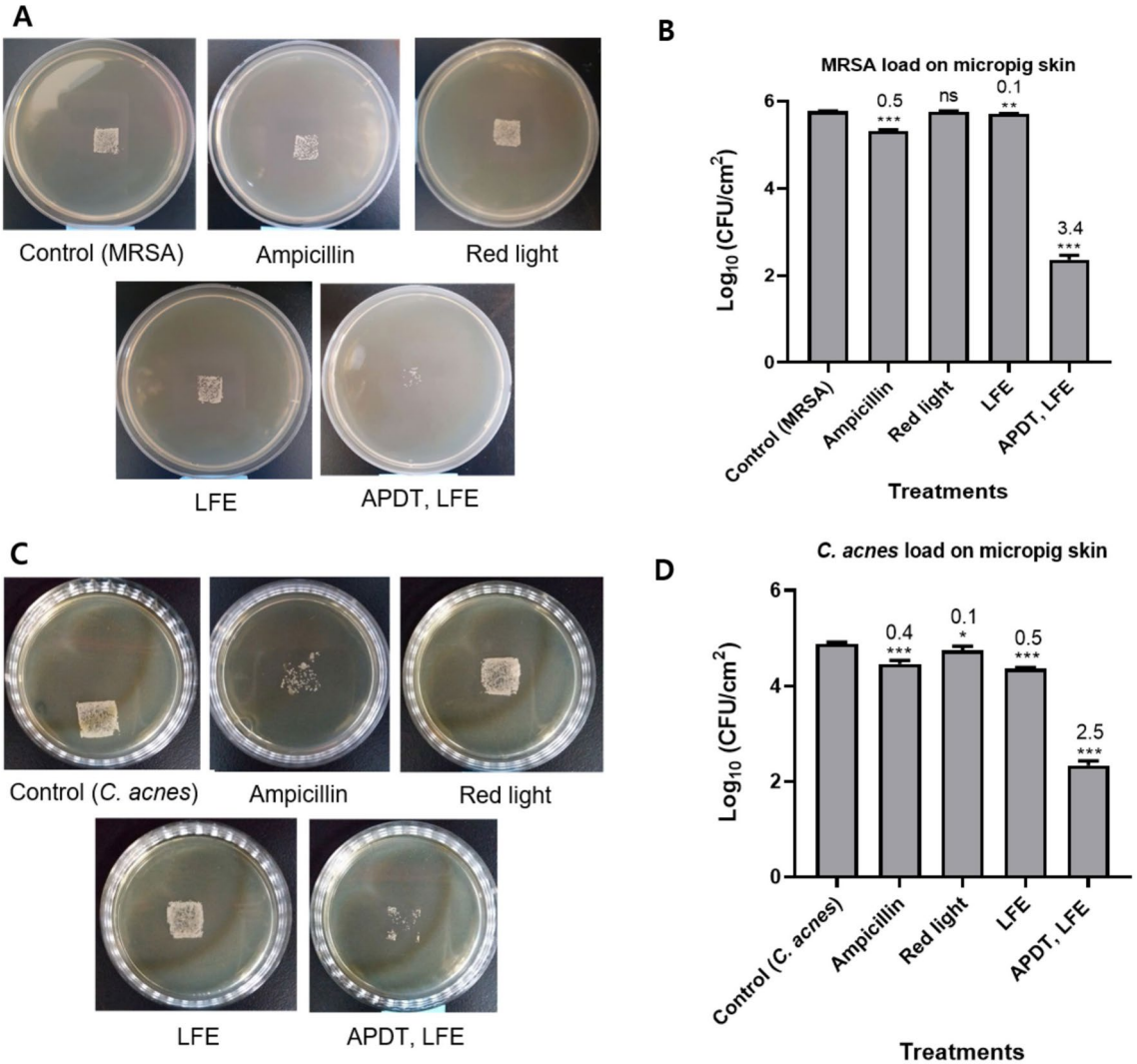

Fig. 8 APDT effects against MRSA and *C. acnes* with LFE on micropig skin. Overnight culture of MRSA or *C. acnes* was incubated with or without LFE (20 µg/mL; 30 min incubation) and spread on the micropig skin at 5 µL/cm^2. Ampicillin (100 µg/mL) was used as a positive control. The coated skin was then illuminated under red light at 20 W/m^2 for 30 min. The treated skin was imprinted on BHI agar to illustrate the inhibition of *C. acnes* or MRSA on the surface of the skin by APDT. Representative images of MRSA growth on LB plates (**A**) and *C. acnes* growth on BHI plates (**C**) were recorded after 48-hour incubation. The differently treated skins were also washed with phosphate-buffered saline using a swab. The total content of bacteria on the swab of each treatment was plated on LB or BHI agar plates. **B**, **D**) CFU formation after 48 h was quantified and represented in the graph as a log (CFU/cm^2). The data are reported as mean ± standard error (n = 2) and representative of at least two independences. ns indicates no statistical significance relative to the control group. Significant differences are expressed with * for $p < 0.05$, ** for $p < 0.01$, and *** for $p < 0.001$ relative to the vehicle control. The log reductions compared with vehicle control are presented in each column

worms. *C. elegans*, an invertebrate model with ease in experimental manipulation, short lifespan, and no ethical concerns, was successfully used as a long-term and quick screening tool for APDT efficacy [16]. *C. elegans* can be used to learn more about the molecular mechanisms of pathogen-host interaction. The assay using micropig skin attempts to simulate the actual cellular infections, given that the binding of photosensitizer at proper doses is critical for effective APDT. Our approach to discover new APDT methods using in vitro, *C. elegans*, and micropig skin promotes a screening platform without live mammalian animal experiments.

Despite the satisfactory photodynamic antimicrobial effects in vitro and in vivo nematode model, our study carries some limitations. In our linked study, wound healing effect of LFE phototreatment in a rodent model would highlight the utility of the existing APDT approach in treating various infectious diseases in

mammalian systems. However, bioassays for the underlying effect of ROS on pathogen virulence factors are lacking. The tested bacterial collection is well known for its ability to produce biofilms, which mediate pathogen adhesion and dissemination to host cells, allowing pathogens to spread broadly and prolong the infection. Biofilms are less responsive to antimicrobial therapy due to extracellular matrix components and quorum sensing [43]. Therefore, further research into the biofilm inhibitory effects of APDT with LFE is required. Moreover, infectious conditions may be caused by a diverse community of pathogens. Therefore, a multi-species infections simulation model should be established to offer insight into the action of APDT.

The present study revealed that the treatment of LFE with red light showed a substantial inhibitory effect against MRSA and common pathogenic bacteria involved in infectious diseases. Taken together with the therapeutic effects of increasing survival and reversing growth retardation under infection in *C. elegans* model, we foresee that LFE holds excellent promise as a new photosensitizer source for the antimicrobial photodynamic treatment of MRSA infectious diseases in this post-antibiotic era. However, in-depth studies on the underlying mechanism of bacterial cell death caused by APDT and the interaction of pathogen-host-APDT in mammalian models are required to guarantee its efficacy and safety in clinical settings.

Abbreviations

APDT	Antimicrobial photodynamic therapy
BHI	Brain heart infusion
CFU	Colony-forming unit
HPLC	High-pressure liquid chromatography
LB	Luria-Bertani
LED	Light emitting diode
LFE	*Ligulariafischeri* extract
MRSA	Methicillin-resistant *Staphylococcus aureus*
MS	Mass spectrometry
NGM	Nematode growth medium
NMR	Nuclear magnetic resonance
ROS	Reactive oxygen species
UPLC	Ultra-performance liquid chromatography

Supplementary Information

The online version contains supplementary material available at https://doi.org/10.1186/s13765-023-00778-2.

Additional file 1: The ^{1}H NMR and MS data of compounds 1-3. **Fig. S1** Relative singlet oxygen generation of 50 different plant extracts. 49: *Ligularia fischeri*. **Fig. S2** Relative singlet oxygen generation of LFE and fractions (F1-F4). **Fig. S3** APDT of LFE and fractions against MRSA. APDT with LFE and fractions (F1-F4) (20 μg/mL, 30 min incubation) against MRSA under red light (660 nm) with the intensity of 20 W/m^2 for 30 min. Ampicillin (100 μg/mL) served as the positive control. The data are expressed as mean ± standard error (n = 2) and representative of three independences. ns indicates no statistical significance relative to the control group. Significant differences are expressed with *** for $p < 0.001$ relative to the vehicle control. The log reductions compared with vehicle control are presented in each column. **Fig. S4** Effects of APDT efficacy on lifespan (A) and bacterial attachment (B) in *S. aureus* KCTC3881 and infected *C. elegans*. Adult *C. elegans* were treated with overnight *S. aureus* culture for a day. Then, LFE (20 μg/mL) was treated for 30 min. DMSO was used as the control group. Next, the worms were allowed to crawl to blank NGM agar twice before the irradiation to red light (600 W/m^2 for 5 min). The worms were then assessed for survivability every day (A). The p-value according to the *S. aureus* single treatment is presented. The results are representative of three independent experiments. Five worms from each treatment plate were also moved to fresh LB broth and spread onto LB agar for CFU determination of viable bacteria associated with *C. elegans* (B). The data are reported as mean ± standard error of duplicates and representative of three independent experiments. ns indicates no statistical significance relative to *S. aureus*; significant differences are expressed with ** for $p < 0.01$ and *** for $p < 0.001$ relative to *S. aureus*. The log reductions compared with *S. aureus* are presented in each column.

Acknowledgements
The *Caenorhabditis elegans* strains were provided by the *Caenorhabditis* Genetics Center (Minneapolis, MN, USA).

Author contributions
Conceptualization: HK, JK, and KK; Methodology: NMH, HH, STA, UTTN, SL, JK, and KK; Investigation: NMH, STA, HH, SL, UTTN, JK; Resources: HH, SL, JP, JK, and HK; Supervision: JK and KK; Writing: NMH, JK, and KK. All authors read and approved the final manuscript.

Funding
This work was supported by an intramural research grant from KIST (2E32611, 2E31881) and a grant from the Ministry of Trade, Industry and Energy (MOTIE, Republic of Korea, 20008861).

Availability of data and materials
All data generated or analysed during this study are included in this published article and its Additional files.

Declarations

Competing interests
The authors declare that they have no competing interests.

Received: 10 December 2022 Accepted: 26 February 2023
Published online: 13 March 2023

References

1. Pendleton JN, Gorman SP, Gilmore BF (2013) Clinical relevance of the ESKAPE pathogens. Expert Rev Anti Infect Ther 11(3):297–308
2. Ochsner M (1997) Photophysical and photobiological processes in the photodynamic therapy of tumours. J Photochem Photobiol B 39(1):1–18
3. Hamblin MR (2016) Antimicrobial photodynamic inactivation: a bright new technique to kill resistant microbes. Curr Opin Microbiol 33:67–73
4. Kashef N, Hamblin MR (2017) Can microbial cells develop resistance to oxidative stress in antimicrobial photodynamic inactivation? Drug Resist Updat 31:31–42
5. Tomb RM, Maclean M, Coia JE, MacGregor SJ, Anderson JG (2017) Assessment of the potential for resistance to antimicrobial violet-blue light in Staphylococcus aureus. Antimicrob Resist Infect Control 6:100
6. Polat E, Kang K (2021) Natural photosensitizers in antimicrobial photodynamic therapy. Biomedicines 9(6):584
7. Lee KH, Choi EM (2008) Analgesic and anti-inflammatory effects of *Ligularia fischeri* leaves in experimental animals. J Ethnopharmacol 120(1):103–107

8. Hong S, Joo T, Jhoo J-W (2015) Antioxidant and anti-inflammatory activities of 3,5-dicaffeoylquinic acid isolated from *Ligularia fischeri* leaves. Food Sci Biotechnol 24(1):257–263
9. Dilberger B, Weppler S, Eckert GP (2021) Phenolic acid metabolites of polyphenols act as inductors for hormesis in *C. elegans*. Mech Ageing Dev 198:111518
10. Xie Z, Zhao J, Wang H, Jiang Y, Yang Q, Fu Y et al (2020) Magnolol alleviates Alzheimer's disease-like pathology in transgenic *C. elegans* by promoting microglia phagocytosis and the degradation of beta-amyloid through activation of PPAR-γ. Biomed Pharmacother 124:109886
11. Dimitriadi M, Hart AC (2010) Neurodegenerative disorders: insights from the nematode *Caenorhabditis elegans*. Neurobiol Dis 40(1):4–11
12. Shen P, Zhang R, McClements DJ, Park Y (2019) Nanoemulsion-based delivery systems for testing nutraceutical efficacy using *Caenorhabditis elegans*: demonstration of curcumin bioaccumulation and body-fat reduction. Food Res Int 120:157–166
13. Lee M, Youn E, Kang K, Shim YH (2022) 3,3'-Diindolylmethane supplementation maintains oocyte quality by reducing oxidative stress and CEP-1/p53-Mediated regulation of germ cells in a reproductively aged *Caenorhabditis elegans* model. Antioxidants. 11(5):950
14. Kim JY, Le TAN, Lee SY, Song DG, Hong SC, Cha KH et al (2019) 3,3'-Diindolylmethane improves intestinal permeability dysfunction in cultured human intestinal cells and the model animal *Caenorhabditis elegans*. J Agric Food Chem 67(33):9277–9285
15. Kim MR, Cho SY, Lee HJ, Kim JY, Nguyen UTT, Ha NM et al (2022) Schisandrin C improves leaky gut conditions in intestinal cell monolayer, organoid, and nematode models by increasing tight junction protein expression. Phytomedicine 103:154209
16. Ha N, Tran S, Shim Y-H, Kang K (2022) *Caenorhabditis elegans* as a powerful tool in natural product bioactivity research. J Appl Biol Chem 65:1
17. Kim JY, Lee SY, Jung S-H, Kim MR, Choi I-D, Lee J-L et al (2020) Protective effect of *Lactobacillus casei* HY2782 against particulate matter toxicity in human intestinal CCD-18Co cells and *Caenorhabditis elegans*. Biotechnol Lett 42(4):519–528
18. Lee SY, Kang K (2017) Measuring the effect of chemicals on the growth and reproduction of *Caenorhabditis elegans*. J Vis Exp. https://doi.org/10.3791/56437
19. Alam ST, Hwang H, Son JD, Nguyen UTT, Park JS, Kwon HC et al (2021) Natural photosensitizers from *Tripterygium wilfordii* and their antimicrobial photodynamic therapeutic effects in a *Caenorhabditis elegans* model. J Photochem Photobiol B 218:112184
20. Alam ST, Le TAN, Park JS, Kwon HC, Kang K (2019) Antimicrobial biophotonic treatment of ampicillin-resistant *Pseudomonas aeruginosa* with hypericin and ampicillin cotreatment followed by orange light. Pharmaceutics 11(12):641
21. Singh S, Fatima Z, Ahmad K, Hameed S (2020) Repurposing of respiratory drug theophylline against *Candida albicans*: mechanistic insights unveil alterations in membrane properties and metabolic fitness. J Appl Microbiol 129(4):860–875
22. Le TAN, Selvaraj B, Lee JW, Kang K (2019) Measuring the effects of bacteria and chemicals on the intestinal permeability of *Caenorhabditis elegans*. J Vis Exp. https://doi.org/10.3791/60419
23. Moy TI, Conery AL, Larkins-Ford J, Wu G, Mazitschek R, Casadei G et al (2009) High-throughput screen for novel antimicrobials using a whole animal infection model. ACS Chem Biol 4(7):527–533
24. De Magalhaes Filho CD, Henriquez B, Seah NE, Evans RM, Lapierre LR, Dillin A (2018) Visible light reduces *C. elegans* longevity. Nat Commun 9(1):927
25. Stolik S, Delgado JA, Pérez A, Anasagasti L (2000) Measurement of the penetration depths of red and near infrared light in human "ex vivo" tissues. J Photochem Photobiol B 57(2–3):90–93
26. Tonomura S, Ihara M, Kawano T, Tanaka T, Okuno Y, Saito S et al (2016) Intracerebral hemorrhage and deep microbleeds associated with cnm-positive *Streptococcus mutans* a hospital cohort study. Sci Rep 6:20074
27. Douglas LJ (2003) Candida biofilms and their role in infection. Trends Microbiol 11(1):30–36
28. Turner NA, Sharma-Kuinkel BK, Maskarinec SA, Eichenberger EM, Shah PP, Carugati M et al (2019) Methicillin-resistant *Staphylococcus aureus*: an overview of basic and clinical research. Nat Rev Microbiol 17(4):203–218
29. Chan BCL, Dharmaratne P, Wang B, Lau KM, Lee CC, Cheung DWS et al (2021) Hypericin and pheophorbide a mediated photodynamic therapy fighting MRSA wound infections: a translational study from in vitro to in vivo. Pharmaceutics 13(9):1399
30. Tanielian C, Kobayashi M, Wolff C (2001) Mechanism of photodynamic activity of pheophorbides. J Biomed Opt 6(2):252–256
31. Campanholi KdSS, Gerola AP, Vilsinski BH, de Oliveira ÉL, de Morais FAP, Rabello BR et al (2018) Development of Pluronic® nanocarriers comprising pheophorbide, Zn-pheophorbide,;apachol and β-lapachone combined drugs: Photophysical and spectroscopic studies. Dyes Pigm 157:238–250
32. Gerola AP, Santana A, França PB, Tsubone TM, de Oliveira HP, Caetano W et al (2011) Effects of metal and the phytyl chain on chlorophyll derivatives: physicochemical evaluation for photodynamic inactivation of microorganisms. J Photochem Photobiol 87(4):884–894
33. Alhenaki AM, Alqarawi FK, Tanveer SA, Alshahrani FA, Alshahrani A, AlHamdan EM et al (2021) Disinfection of acrylic denture resin polymer with Rose Bengal, Methylene blue and porphyrin derivative in photodynamic therapy. Photodiagnosis Photodyn Ther 35:102362
34. Song BH, Lee DH, Kim BC, Ku SH, Park EJ, Kwon IH et al (2014) Photodynamic therapy using chlorophyll-a in the treatment of acne vulgaris: a randomized, single-blind, split-face study. J Am Acad Dermatol 71(4):764–771
35. Hirt HM, M'Pia B (2008) Natural medicine in the tropics 1: Foundation text. Anamed, Winnenden
36. Patra JK, Das G, Lee S, Kang S-S, Shin H-S (2018) Selected commercial plants: a review of extraction and isolation of bioactive compounds and their pharmacological market value. Trends Food Sci Technol 82:89–109
37. Park CH, Ahn MJ, Hwang GS, An SE, Whang WK (2016) Cosmeceutical bioactivities of isolated compounds from *Ligularia fischeri* Turcz leaves. Appl Biol Chem 59(3):485–494
38. Zeina B, Greenman J, Purcell WM, Das B (2001) Killing of cutaneous microbial species by photodynamic therapy. Br J Dermatol 144(2):274–278
39. Demidova TN, Hamblin MR (2005) Effect of cell-photosensitizer binding and cell density on microbial photoinactivation. Antimicrob Agents Chemother 49(6):2329–2335
40. Pietrowska A, Hołowacz I, Ulatowska-Jarża A, Guźniczak M, Matczuk AK, Wieliczko A et al (2022) The enhancement of antimicrobial photodynamic therapy of *Escherichia coli* by a functionalized combination of photosensitizers: in vitro examination of single cells by quantitative phase imaging. Int J Mol Sci 23(11):6137
41. Li WT, Tsao HW, Chen YY, Cheng SW, Hsu YC (2007) A study on the photodynamic properties of chlorophyll derivatives using human hepatocellular carcinoma cells. Photochem Photobiol Sci 6(12):1341–1348
42. Samaranayake YH, Samaranayake LP (2001) Experimental oral candidiasis in animal models. Clin Microbiol Rev 14(2):398–429
43. Costerton JW, Stewart PS, Greenberg EP (1999) Bacterial biofilms: a common cause of persistent infections. Science 284(5418):1318–1322

Publisher's Note